Effect of acupuncture on the autonomic nervous system as evaluated by non-contact heart rate variability measurement

Kouki Kurita*1, Kaoru Kiyomitsu*1, Chie Ogasawara*2, Rei Mishima*2, Keiko Ogawa-Ochiai*2 and Norimichi Tsumura*1

1 *Graduate School of Advanced Integration Science, Chiba University, 1-33 Yayoi-cho, Inage-ku, Chiba 263-8522, Japan*

2 *Department of Japanese-Traditional (Kampo) Medicine, Kanazawa University Hospital, Kanazawa, Japan*

e-mail:k.kurita57@gmail.com

Abstract: We evaluated the effect of acupuncture treatment on the autonomic nervous system by measuring the non-contact heart rate variability (HRV). HRV shows the changes in sympathetic and parasympathetic nervous activities. Sympathetic and parasympathetic nervous activities are respectively reflected in the high frequency (HF) and low frequency (LF) components of HRV. Many studies have shown that sensory stimulation affects the cardiovascular system. In particular, acupuncture stimulation often decreases the LF component, and there is a significant positive correlation between the HF component and the number of acupuncture sensations administered. These previous studies generally used an electrocardiograph or other contact plethysmograph to obtain the HRV. However, the use of electrodes and contact sensors might cause the participants to experience stress. Therefore, we used non-contact HRV measurement to evaluate the effect of acupuncture treatment. Using a remote measurement system with a digital camera enables the exclusion of external factors, and the attainment of more natural biological information. In the present study, we verified the accuracy of remote HRV measurement using a digital camera, and evaluated the effect of acupuncture on the autonomic nervous system.

Keywords: image analysis, acupuncture, heart rate variability (HRV), remote HRV measurement

1 INTRODUCTION

The autonomic nervous system is affected by sensory stimuli such as vision, tactile sensations, pain sensations, and warming sensations. Acupuncture treatment reportedly often decreases the low frequency (LF)/high frequency (HF) ratio of heart rate variability (HRV). Previous studies have evaluated the sympathetic nervous activity after acupuncture using electrocardiography, plethysmography, or changes in skin temperature or blood pressure. However, the LF and HF components of HRV can be calculated using power spectral analysis; these components reflect the activities of the sympathetic and parasympathetic nervous systems, respectively. Sato et al. [1] assessed the effect of acupuncture on HRV using electrocardiography. However, contact monitoring is not easily accepted by the participants, as they may feel some discomfort while being touched. Using a remote measurement system can exclude the effect of such external factors.

Remote heart rate (HR) measurement has already become popular. There are various techniques used to measure blood volume pulse (BVP); for example, Verkruysse et al. [2] measured the BVP using ambient light. Furthermore, frontier work has made it possible to remotely measure cardiopulmonary parameters (HR, respiratory rate (RR), and the HF and LF components of HRV) [3]. HRV is a useful non-invasive measurement of phenomena such as the modulation of the sympathetic nervous system. However, this index requires the acquisition of pulse wave signals with a much greater degree of accuracy compared with HR and RR.

Fig. 1 Original image

Our previous research achieved a high degree of accuracy in the measurement of HRV [4]. The method used involved the application of pigment component separation to a RGB facial image to obtain the hemoglobin, melanin, and shading components of the image [5]. Fig. 1 and 2 show the results of skin pigment component separation. Hemoglobin pigments are circulated in the face via the bloodstream, and the hemoglobin concentration of the surface of the face temporarily increases with the BVP. Hence, using the extracted hemoglobin images can reduce noise factors and thus enable the calculation of HRV with a high degree of accuracy.

In the present study, we used this remote HRV measurement system to evaluate the effect of acupuncture treatment. Obtaining the BVP signal without using any contact sensors enabled the examination of participants in a natural condition. In section 2, we described the method used to obtain the BVP. In section 3, we verified the accuracy of measuring the HRV using the camera method compared with an electrocardiograph. In sections 4 and 5, we described an experiment in which acupuncture treatment was applied without electrocardiography.

2 Extraction of Hemoglobin Information from a Color Facial Image [5]

The human skin can be broadly categorized into two principal layers: the epidermis and the dermis. The epidermis contains melanin pigments, while the dermis contains hemoglobin pigments. Incident light into the skin passes through the epidermis and dermis, and is subsequently emitted to the outside from the skin surface. The modified Lambert-Beer law is presumptively satisfied in the skin layer for incident light. It is conceivable that incident light is absorbed by the hemoglobin pigments and melanin pigments. The skin color depends on the distribution of these two pigments. Based on this assumption, we extracted the hemoglobin pigments, melanin pigments, and shading from skin color images using independent component analysis. In Fig. 3, $\boldsymbol{v}^{\log}$ is the obtained density distribution signal calculated using the converted logarithm, and is represented by the weighted linear combination of the three vectors ($\boldsymbol{\sigma}_{h}$, $\boldsymbol{\sigma}_{h,}$, and $\boldsymbol{1}$) with the bias vector $\boldsymbol{e}^{\log}$. The vectors $\boldsymbol{\sigma}_{h}$ and $\boldsymbol{\sigma}_{h,}$ are the relative absorbance vectors for the hemoglobin and melanin components, respectively, while the vector $\boldsymbol{1}$ is the shading vector. Fig. 2a and 2b show the extracted hemoglobin and melanin pigments, while Fig. 2c shows the shading obtained by independent component analysis of the whole facial image shown in Fig. 1.

As the subject in the figure is Japanese, and the dominant type of melanin in Japanese subjects is eumelanin, this figure enabled the estimation of the eumelanin component. The eumelanin component was also shown in the hair region, as the subject in the figure has black hair, and the dominant type of melanin in black hair is eumelanin.

The accuracy of the pigment estimation (physiological validity) was confirmed using the same techniques described in a previous study [5]. The arm of a subject was irradiated by UV-B for the analysis of the melanin component, while methyl nicotinate was applied to the other arm for the hemoglobin component, as methyl nicotinate is known to increase the hemoglobin content [5]. A similar analysis of the respective images in the present study confirmed that the melanin and hemoglobin components were separated with good physiological validity.

(a) Hemoglobin component

(b) Melanin component

(c) Shading

Fig. 2 The results of skin color separation

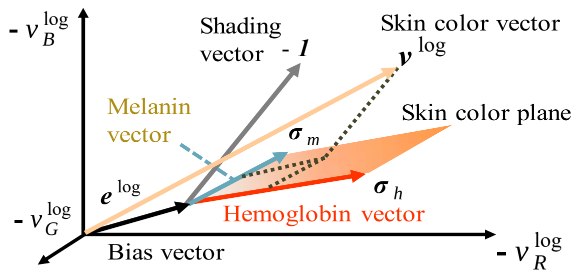

Fig. 3 Overview of skin color separation

In the present study, the modified Lambert-Beer law was used for the approximation for the imaging model, similarly to the method used in a previous study [5]. The modified Lambert-Beer law is based on the mean path length, which is affected by the scattering from skin tissue. Therefore, the influence of scattering was included in the present analysis.

3 Extracting the Blood Volume Pulse Signal from Video Images

The method described in section 2 was used to obtain the hemoglobin component images shown in Fig. 2a from the video images captured by the camera. These hemoglobin images represent the temporal fluctuation of the hemoglobin concentration of the facial surface, and were used to obtain the BVP. However, these images included the artifacts of blinking and eye movements. Therefore, we set the region of interest (ROI) to the area around the cheek. The size of the ROI changed depending on each participant, as the ROI was set to exclude the eye, ear, and mouth while including an area of more than 100 × 100 pixels on the cheek. The frame rate of the camera was 30 fps in these experiments.

We calculated the average values of the pixels in the ROI. Fig. 4 shows the temporal change of the average pixel values. The component of the HR was detected in this signal. We applied detrending [6] and band-pass filtering to this signal to easily enable the detection of peaks. We used a technique based on the smoothness prior approach to detrend the signals. This signal was band-pass filtered using a Hamming window filter with respective LF and HF cut-offs of 45 beats/minute (0.75 Hz) and 180 beats/minute (3 Hz). These cut-off frequencies were decided based on the lower and upper limits of the HR. Fig. 5 shows the BVP signal obtained by these processes.

4 Verifying the Accuracy of Remote Heart Rate Variability Measurement

We used the simple peak detection method. The local peaks of the BVP waveform were detected by comparing the signal value of the waveform with the neighboring values, based on the hill climbing method. The peaks of the electrocardiogram waveform shown in Fig. 6 are called R waves, and correspond with the peaks of the BVP signal. The interval between R waves is called the R-R interval. The R-R intervals are continually fluctuating. Therefore, we constructed the HRV graph shown in Fig. 7 and 8 by calculating the power spectral density from the R-R intervals using a Lomb periodogram [7].

The HF (0.15–0.4 Hz) signals reflect the parasympathetic influence on the HR, and are correlated to respiratory sinus arrhythmia. In contrast, the LF (0.05–0.15 Hz) signals are modulated by blood pressure fluctuation, and reflect both sympathetic and parasympathetic activities [8].

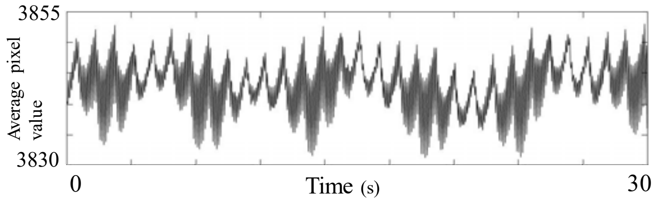

Fig. 4 Average pixel value of the hemoglobin component image

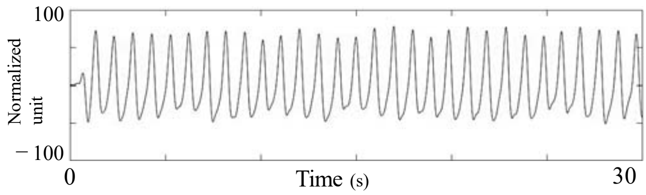

Fig. 5 The signal after normalization, detrending, and filtering.

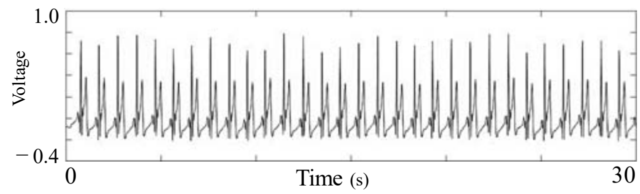

Fig. 6 Electrocardiogram

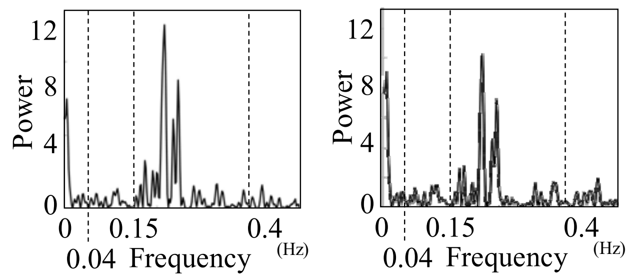

(a) Electrocardiogram (b) Camera

Fig.7 Power spectral density of participant 1

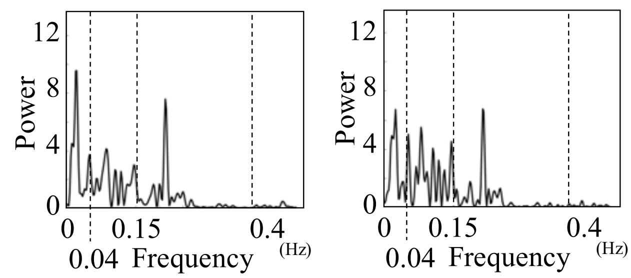

(a) Electrocardiogram (b) Camera

Fig.8 Power spectral density of participant 2

The sympathetic modulation can be estimated by considering the LF/HF ratio. For example, when the subject is relaxed, the parasympathetic nervous system becomes activated. Parasympathetic nerves influence HF signals. Fig. 7a and 7b show the HRV; there was a large spectrum at the HF range, and a small spectrum at the LF range (Fig. 7). These results indicate that participant 1 was relaxed. In contrast, when a subject is experiencing stress, the sympathetic nerves become activated. Sympathetic nerves make the heart less likely to be affected by respiratory sinus arrhythmia. Therefore, the LF/HF ratio decreases compared with that seen in a subject in a relaxed state. In Fig. 8a and 8b, the HRV spectrum at the HF range decreased, and the integrated value at the LF range exceeded that of the HF range. These results indicate that that participant 2 was experiencing stress. Table 1 shows the results of participants 1 and 2. HR was calculated as 60 divided by the mean R-R interval. The RR shows the frequency when the highest peak value was acquired in the HF range. LF and HF were calculated as the integrated values of each range. These results indicate that the camera method reproduced the values obtained using the electrocardiograph with a high degree of accuracy. Thus, this method can be used to determine whether participants are relaxed or stressed, without using contact sensors. We then applied this method to evaluate the effect of acupuncture treatment on HRV.

Table 1 Summary of the results in Fig. 7 and 8 using the values of the heart rate (HR; bpm), respiratory rate (RR; bpm), and the low frequency (LF)/high frequency (HF) ratio before and after acupuncture treatment

		HR	RR	LF/HF
Partcipant1	ECG	60.5	13.0	0.13
	Camera	60.5	13.0	0.18
Participant2	ECG	58.6	12.8	1.33
	Camera	58.7	12.8	1.44

5 Evaluating the Effect of Acupuncture using a Camera

The present experiments were performed on three participants. The participants were males aged 20–40 years; these were two Japanese students and one Professor of Chiba University.

The specific acupuncture protocols employed in the present study are described below. Point locations were as described in standard textbooks. Disposable sterile silver needles (0.16 × 24 mm) were positioned on the skin and left in place for 30 seconds to 1 minute without being inserted. Acupuncture was performed in all cases by the same senior

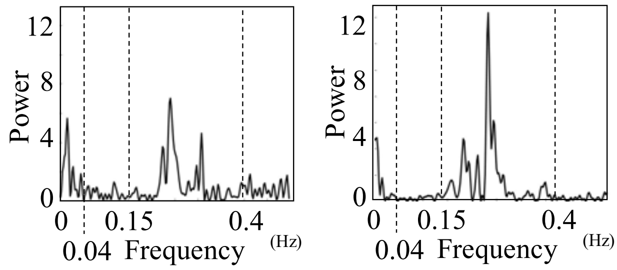

(a) Pre-acupuncture (b) Post-acupuncture

Fig. 9 Power spectral density of participant 1

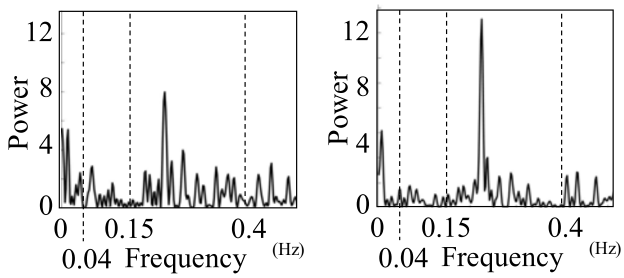

(a) Pre-acupuncture (b) Post-acupuncture

Fig. 10 Power spectral density of participant 2

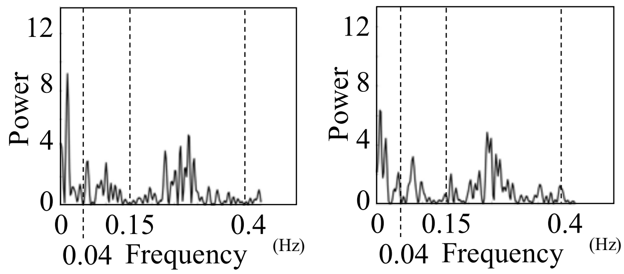

(a) Pre-acupuncture (b) Post-acupuncture

Fig. 11 Power spectral density of participant 3

acupuncturist who had several years of acupuncture experience. Contact needle therapy [9] was performed in accordance with the medical diagnosis for each participant, which was based on meridian therapy. Acupuncture points used for all patients were CV12, CV4, ST25, and KI2; in addition, the following points were used in specific patients: LR8, LR14, SP3, LR13, LU9, LU1, KI7, GB25, PC7, CV17, CV6, CV4, ST36, LU1, BL20, BL13, BL18, and BL23.

The HRV was calculated twice in each participant before and after acupuncture treatment. We used a digital camera to obtain the BVP. Each participant was relaxed and in a reclining position on the examination bed during the experiments. As HRV is strongly affected by changes in posture, the participants lay down for 5 minutes before the start of the measurements, and kept their face up during the experiments. The camera (1/1.8" Sony CMOS Pregius IMX265, DFK33UX265, 2048 × 1536) was positioned at a distance of 3 meters from the participant. Facial videos of each participant were captured while the participants were illuminated by a fluorescent light source.

6 Results

The power spectral HRV results are shown in Fig. 9–11. The post-acupuncture state had a much greater HF component than the pre-acupuncture state. Table 2 shows the HR, RR, LF/HF values before and after acupuncture treatment. The LF/HF values were slightly decreased after acupuncture in all participants, indicating that the participants relaxed during the experiment.

Table 2 Summary of the results shown in Fig. 9, 10, and 11 using the values of heart rate (HR; beats/minute), respiratory rate (RR; breaths/minute), and the ratio of low frequency/high frequency components (LF/HF)

		HR	RR	LF/HF
Partcipant1	Before	59.2	14.4	0.17
	After	56.4	14.0	0.07
Participant2	before	68.4	13.0	0.23
	After	65.4	13.5	0.17
Participant3	before	52.1	16.8	0.43
	After	51.1	14.4	0.30

7 Conclusion and Discussion

HRV can be obtained with a high degree of accuracy using a conventional camera to photograph the subject while he/she is illuminated with a fluorescent light source. Furthermore, we applied this method to evaluate the effect of acupuncture treatment. All participants were less stressed by the non-contact measurement method than by measurement using contact sensors. The LF/HF values were slightly decreased in all participants. The changes in HR, RR, and LF/HF after acupuncture showed in Table 2 were not statistically significant, as there were only three participants. Future studies with larger sample sizes are needed to confirm the present findings.

ACKNOWLEDGMENT

We thanks to Mai Sugawara for her management of the experiments.

REFERENCES

[1] Y. Sato, T. Hanawa, M. Arai, J. -C, Cyong, M. Fukuzawa, et al.: Introduction to KAMPO Japanese Traditional Medicine, Acupuncture and moxibustion, Elsevier Japan K.K., 2005.

[2] W. Verkruysse, L. O. Svaasand and J. S. Nelson: Remote plethysmographic imaging using ambient light, Optics Express, Vol.16, No.26, pp.21434--21445, 2008.

[3] R. E. Kleiger, J. P. Miller, J. T. Bigger Jr. and A. J. Moss: Decreased heart rate variability and its association with increased mortality after acute myocardial infarction, Amer. J. Cardiol., Vol.59, No.4, pp.256--262, 1987.

[4] K. Kurita, T. Yonezawa, M. Kuroshima, N. Tsumura: Non-Contact Video Based Estimation for Heart Rate Variability Spectrogram Using Ambient Light by Extracting Hemoglobin Information, Proc. Color and Imaging Conference, pp.207--211, 2015.

[5] N. Tsumura, N. Ojima, K. Sato, M. Shiraishi, H. Shimizu, H. Nabeshima, S. Akazaki, K. Hori, Y. Miyake: Image-based skin color and texture analysis/synthesis by extracting hemoglobin and melanin information in the skin, ACM Transactions on Graphics, Vol.22, No.3, pp.770--779, 2003.

[6] B. Martinez, M. F. Valstar, X. Binefa and M. Pantic: Local evidence aggregation for regression-based facial point detection, IEEE Trans. Biomed. Eng.}, Vol.49, No.2, pp.172--175, 2002.

[7] W. H. Press, S. A. Teukolsky, W. T. Vetterling and B. P. Flannery: Numerical recipes in Fortran 77: the art of scientific computing, Cambridge University Press},2nd ed. Vol.1, pp.569--577, 2001.

[8] S. Akselrod, D. Gordon, F. A. Ubel, D. C. Shannon, A. Berger and R. J. Cohen: Power spectrum analysis of heart rate fluctuation: A quantitative probe of beat-to-beat cardiovascular control, Science}, Vol.213, No.~4504, pp.220--222, 1981.

[9] K. Ogawa, M. Ogawa, K. Nishijima, M. Tsuda, and G. Nishimura, Efficacy of Contact Needle Therapy for Chemotherapy-Induced Peripheral Neuropathy, Evidence-Based Complementary and Alternative Medicine, Vol. 2013, Article ID 928129, 5 pages http://dx.doi.org/10.1155/2013/928129